AFTSolve: A program for multi-kinetic modeling of apatite fission-track data

Article *in* American Mineralogist · January 2000

3 authors, including:

Richard Ketcham
University of Texas at Austin
258 PUBLICATIONS   **12,061** CITATIONS

SEE PROFILE

Some of the authors of this publication are also working on these related projects:

Rock burst View project

AFTSolve: A program for multi-kinetic modeling of apatite fission-track data

Richard A. Ketcham[1], Raymond A. Donelick[2], and Margaret B. Donelick[3]

[1]Department of Geological Sciences, University of Texas, Austin, TX   78712, USA
<richk@maestro.geo.utexas.edu>,   [2]Donelick Analytical, Inc., 1075 Matson Road, Viola, ID 83872, USA <donelick@apatite.com>,   [3]Department of Geology and Geological Engineering, University of Idaho, Moscow, ID   83844, USA <donelick@apatite.com>

Abstract

AFTSolve is a computer program for deriving thermal history information from apatite fission-track data. It implements a new fission-track annealing model that takes into account the known kinetic variability among different apatite species. To fully utilize this model, a fission-track worker must obtain data that can be used to infer the kinetic characteristics of each apatite grain from which a measurement was taken. Such data can consist of etch figure lengths or chemical composition. The benefit of this overall approach is that it allows useful information to be derived from previously unusable analyses, extends the practical range of geological temperatures constrained by fission-track analyses, and increases overall confidence in model predictions. AFTSolve also incorporates the effects of fission-track orientation relative to the apatite crystallographic c-axis, variation in initial track length, and the biasing effect of ^{252}Cf irradiation for enhancing confined horizontal track length detection. AFTSolve is written for Windows$^{®}$ operating systems, and has a graphical interface that allows interactive input of thermal histories and real-time generation of estimates for fission-track length distributions and ages for up to six simultaneously modeled kinetic populations. It also includes procedures for estimating the range of time-temperature histories that are statistically consistent with a data set.

Introduction

Fission tracks in apatite provide a unique tool for estimating low-temperature thermal histories. Because fission tracks form continuously over time and subsequently anneal (shorten) as a function of time and temperature, the set of track lengths measured for a sample provides an uninterrupted record of the temperatures it has experienced. A number of computer programs have been developed that use this principle to estimate thermal histories based on fission-track data (Corrigan, 1991; Crowley, 1993; Gallagher, 1995; Lutz and Omar, 1991; Willett, 1997).

The basis for all such programs is a calibration that characterizes fission-track annealing as a function of time and temperature (Carlson, 1990; Crowley et al., 1991; Ketcham et al., 1999; Laslett and Galbraith, 1996; Laslett et al., 1987). A significant limitation in most of these calibrations, with the notable exception of Ketcham et al. (1999), is that they typically describe the behavior of a single type of apatite, such as Durango apatite (Green et al., 1986) or an end-member fluorapatite (Crowley et al., 1991). In many cases encountered in nature, especially in sedimentary rocks, the apatites in a sample represent more than one kinetic population; i.e.,

different apatites exhibit different annealing behaviors and different closure temperatures. In such cases, statistical analysis of the single-grain ages often reveals that the data are not derived from a single population. Previously, such a determination precluded rigorous use of the data for thermal history estimation, as it was impossible to determine which measurements, particularly fission-track lengths, corresponded to which apatite kinetic populations. The procedure first introduced by Burtner et al. (1994), in which each apatite from which either a track length or density measurement was taken was also evaluated for its relative resistance to annealing, allows kinetic variation to become a strength rather than a liability. If the apatites measured exhibit a range of closure temperatures, they collectively constrain the time at which the sample passed through each closure temperature represented. Furthermore, they offer parallel, essentially independent, constraints on the thermal history at temperatures below the lowest closure temperature represented.

Forward Model Components

There are three processes that determine the character of measured fission-track data: formation, annealing, and detection. Calculation of the forward model that takes as input a time-temperature (t-T) path and produces an estimated fission-track age and length distribution can be broken out along these lines. We begin with annealing, the equation for which is the centerpiece of any model, and then discuss how formation and detection are taken into account.

Annealing

The primary annealing model implemented by AFTSolve is presented by Ketcham et al. (1999). It is based on a data set of 408 annealing experiments conducted on 15 different types of apatite (Carlson et al., 1999), and a new model that corrects for fission-track length anisotropy with respect to the crystallographic axes of apatite (Donelick et al., 1999). In addition, the final form of the model was chosen based on its ability to replicate two geological benchmarks: down-well measurements from the Otway Basin for annealing of end-member fluorapatite at high temperature (e.g., Green et al., 1989) and an analysis from a deep-sea drill core that has probably had an exclusively low-temperature history since deposition, never rising above 21 ºC for over 100 million years (Vrolijk et al., 1992).

The preferred annealing equation describes the apatite B2 in the Carlson et al. (1999) data set, a chlor-hydroxy apatite from Bamle, Norway, which was the most resistant to annealing of the apatites studied:

$$\frac{\left(\dfrac{1 - r_{c,mod}^{-11.988}}{-11.988}\right)^{-0.12327} - 1}{-0.12327} = -19.844 + 0.38951\left[\frac{\ln(t) + 51.253}{\ln(1/T) + 7.6423}\right], \tag{1}$$

where $r_{c,mod}$ is the modeled reduced length (length normalized by initial length) of a fission track parallel to the apatite crystallographic c-axis (Donelick et al., 1999) after an isothermal annealing

episode at temperature T (Kelvins) of duration t (seconds). Complete details of the derivation of Equation (1) are provided by Ketcham et al. (1999).

In order to directly use Equation (1), each fission-track length measurement must be accompanied by a measurement of its angle with respect to the apatite crystallographic c-axis. AFTSolve implements the method presented in Donelick et al. (1999) that projects the length of a fission track in any arbitrary orientation to an equivalent c-axis-parallel length. However, many fission-track workers may not measure fission-track orientation, and thus Ketcham et al. (1999) provide and AFTSolve implements functions that convert the c-axis-parallel lengths provided by Equation (1) into mean lengths.

Apatites with the composition of the B2 apatite are very rare, and this apatite is significantly more resistant to annealing than the most common variety, near-end-member fluorapatite. Ketcham et al. (1999) found that the reduced length of any apatite can be related to the length of an apatite that is relatively more resistant to annealing, both lengths resulting from identical thermal histories, by means of the equation

$$r_{lr} = \left(\frac{r_{mr} - r_{mr0}}{1 - r_{mr0}} \right)^{\kappa} , \qquad (2)$$

where r_{lr} and r_{mr} are the reduced lengths of the less-resistant and more-resistant apatites, respectively, and r_{mr0} and κ are fitted parameters. The parameter r_{mr0} corresponds to the reduced length of the more-resistant apatite at the precise time-temperature conditions where the reduced length of the less-resistant apatite falls to zero. Using this equation, Ketcham et al. (1999) were able to construct a single model that incorporated all of the different types of apatite in the Carlson et al. (1999) data set, which spanned a range of closure temperatures from 81 ℃ (for end-member hydroxy-apatite) to over 200 ℃ for B2 apatite. Comparisons against models fitted to individual apatites suggested that the error in extrapolating Equation (2) to geological time scales is minor, causing changes in estimated annealing temperatures that are generally less than 5 ℃.

The set of fitted values for r_{mr0} and κ calculated by Ketcham et al. (1999) suggest a further simplification:

$$r_{mr0} + \kappa \cong 1 \qquad (3)$$

Using this approximation, it is possible to describe the behavior of any apatite using Equations (1) and (2) and a value for r_{mr0}. A complete annealing model for apatite could thus be constructed by finding a function that relates measurable parameters (hereinafter termed kinetic parameters), such as etch figure length (D_{par}, measured in µm) or chemical composition [Cl or OH atoms per formula unit (apfu), based on apatite formula $Ca_{10}(PO_4)_6(F,Cl,OH)_2$], to r_{mr0}. Etch figure length can be used to infer kinetic behavior (Burtner et al., 1994; Donelick, 1993; Donelick, 1995) but is not entirely robust. Likewise, no single chemical compositional variable, including Cl content, provides a completely reliable predictor for r_{mr0}. Other less commonly reported compositional variables such as Fe or Mn substituting for Ca can have effects similar in magnitude to those of Cl (Carlson et al., 1999; Ketcham et al., 1999). Despite their shortcomings,

D_{par} and Cl content are probably sufficient for the majority of apatites and Ketcham et al. (1999) suggest the following two equations to characterize r_{mr0} in terms of D_{par} and Cl content for the fifteen apatites they examined:

$$r_{mr0} = 1 - \exp\left[0.647\left(D_{par} - 1.75\right) - 1.834\right] \tag{4a}$$

$$r_{mr0} = 1 - \exp\left\{2.107\left[1 - \text{abs}\left(Cl - 1\right)\right] - 1.834\right\} \tag{4b}$$

Finally, in addition to estimating the length of a fission-track population after an annealing episode, it is also necessary to estimate the natural spread of lengths that will be observed. Figure 1 shows two functions that estimate the standard deviation of the distribution of track lengths as a function of mean length and c-axis-projected length. Because a significant portion of the spread in track lengths observed in annealing experiments is attributable to anisotropy, estimated errors for determinations of c-axis-projected length are much smaller. In addition, the assumption often made by computer models of a normal distribution of fission-track lengths is more valid about the c-axis-projected mean length than it is about the mean unprojected length; the acceleration of track shortening at relatively high angles to the c-axis at the advanced stages of annealing produces very asymmetrical, even bimodal, distributions about the unprojected mean (Donelick et al., 1999).

Formation

Fission tracks in apatite form continuously over time at a rate dependent solely upon the concentration of uranium present. Earlier-formed fission tracks will tend to be shorter than later-formed tracks, as they will have had more time to anneal, and may have experienced higher temperatures. The distribution of fission-track lengths observed in a sample represents a summation of all of the tracks formed and annealed during its residence below the total annealing temperature. For a given time-temperature history, AFTSolve approximates continuous track formation by subdividing the t-T path into discrete steps, calculating the amount of annealing in the population formed during each time interval over the course of the subsequent t-T history, and summing the populations together.

The optimal time step size to achieve a desired solution accuracy was examined in detail by Issler (1996), who found that time steps must be smaller as the total annealing temperature of apatite is approached. AFTSolve implements a scheme based in part on Issler's (1996) approach, in which solutions obtained using various time step sizes were compared to ones obtained using arbitrarily small time steps. The annealing model depicted by Equation (1) permits larger time steps than the equation studied by Issler (1996), and better than 0.1% precision if no time step has a temperature change of more than 8 °C. When Equation (2) is used convert model results to F-apatite, time steps required are somewhat smaller, but 0.5% precision is assured if there is no step with greater than a 3.5 °C change within 10 °C of the total annealing temperature of F-apatite. The total annealing temperature (T_A) for F-apatite, as defined by Equations (1), (2), and (3) with a r_{mr0} value of 0.84, for a given heating or cooling rate (R) is given by the equation

$$T_A = 377.67\,R^{0.019837}, \tag{5}$$

where T_A is in Kelvins and R is in Kelvins/Ma. AFTSolve subdivides the t-T paths into 100 evenly spaced time steps, interpolating additional steps as necessary to obey the above limitations.

Carlson et al. (1999) also found that initial induced fission-track length varies by more than a micron among different types of apatite. Such a variation can have a significant effect on attempts to replicate low-temperature annealing histories, and should be accounted for in any rigorous modeling effort. Carlson et al. (1999) found that initial length can be roughly predicted using the kinetic indicators D_{par} and Cl content, and provide appropriate functions. These functions are provided in AFTSolve, but it should be noted that their coefficients will almost certainly change with every fission-track worker, especially if the etching technique employed is different from that reported in Carlson et al. (1999). Thus, the program allows the user to change the coefficients as necessary. Alternatively, the user can also specify a single initial length to apply to all apatites.

In either of the cases cited above, the initial length provided to AFTSolve should properly be the initial induced fission-track length, as measured by the worker whose data is to be modeled. Earlier calibrations (e.g., Laslett et al., 1987) predict insufficient annealing at low temperatures, leading to incorrect late-stage thermal histories in many cases unless an artificially low initial track length is used. However, the Ketcham et al. (1999) calibration was selected in part to avoid this shortcoming.

Detection

After the annealed lengths of the fission track populations formed at each time step are calculated, they are summed together using a weighting procedure that takes into account relative track generation within each time step, observational bias, and relative track retention.

The number of tracks formed during a time step is a function of the length of the time interval and the relative concentration of uranium. In young samples the concentration of uranium can be approximated as being constant through time but as sample age increases the depletion due to radioactive decay becomes increasingly significant. For example, uranium concentration and thus fission track production in any given apatite was 1% higher 64.2 m.y. ago than it is at present. The weighting for each time step is the product of its duration and the average relative uranium concentration:

$$w(n) = (t_2 - t_1)\frac{\int_{t_1}^{t_2} e^{\lambda t}\, dt}{t_2 - t_1} = \left(e^{\lambda t_2} - e^{\lambda t_1}\right)/\lambda \,, \tag{6}$$

where time step n is bounded by times t_1 and t_2, in m.y. before present, and λ is the total decay constant for ^{238}U in Ma^{-1}.

The observational bias quantifies the relative probability of observation among the different fission-track populations calculated by the model. Highly annealed populations are less likely to

be detected and measured than less-annealed populations for two primary reasons. First, shorter tracks are less frequently impinged and thus etched (e.g., Laslett et al., 1982). Second, at advanced stages of annealing tracks at high angles to the c-axis may be lost altogether, even though lower-angle tracks remain long; thus the number of detectable tracks in the more-annealed population diminishes, at a rate disproportionate to measured mean length. These two factors can be approximated in a general way by using an empirical function that relates measured fission-track length to fission-track density (e.g., Green, 1988). For example, the model of Willett (1997) uses a fit to the Green (1988) data. AFTSolve uses the model of fission-track length anisotropy presented by Donelick et al. (1999) that closely fits the Green (1988) data and incorporates projection of fission-track lengths onto the crystallographic c-axis:

$$\rho = 1.600 r_{c,\mathrm{mod}} - 0.600, \quad r_{c,\mathrm{mod}} \geq 0.765 ; \tag{7a}$$

$$\rho = 9.205 r_{c,\mathrm{mod}}^2 - 9.157 r_{c,\mathrm{mod}} + 2.269, \quad r_{c,\mathrm{mod}} < 0.765 , \tag{7b}$$

where ρ is normalized fission-track density, which is used as a proxy for observational frequency. Length biasing was neglected in the model of Lutz and Omar (1991).

[252]Cf irradiation of apatite can be a useful technique for increasing the number of confined fission tracks available for length measurement (Donelick and Miller, 1991). However, it can also change the biasing of track detection. Thus, if it is necessary to calculate mean rather than c-axis-projected lengths, we use the empirical functions provided by Ketcham et al. (1999) for experiments with and without Cf-irradiation:

$$r_{\mathrm{m,Cf}} = 1.396 r_{c,\mathrm{mod}} - 0.4017 \tag{8a}$$

$$r_{\mathrm{m,non-Cf}} = -1.499 r_{c,\mathrm{mod}}^2 + 4.150 r_{c,\mathrm{mod}} - 1.656 \tag{8b}$$

Finally, because very short fission tracks are undetectable, they should be eliminated from model results. AFTSolve assumes a minimum detectable length of 2.18 μm, or a reduced length of 0.13, the shortest track observed in over 38,000 measurements in the Carlson et al. (1999) data set.

In addition to the track length distribution, AFTSolve must also predict the pooled fission-track age that would be measured for a particular t-T path. This is calculated by assuming that each time step of length Δt will contribute Δt to the total fission-track age, modified by the amount of track density reduction of the population in that time step relative to the age standard (Willett, 1992). The total age is then the sum of the contributions of each population:

$$age = \frac{1}{\rho_{st}} \sum_i \rho_i \Delta t_i , \tag{9}$$

where ρ_{st} is the estimated fission-track density reduction in the age standard, ρ_i is the fission-track density reduction in the population for time step i, and Δt_i is the duration of time step i. The density reduction in the age standard is calculated using its estimated track length reduction, using the assumption that density reduction is proportional to length reduction, and

that spontaneous fission tracks are initially as long as induced tracks. For example, if for a fission-track worker the Durango apatite has a measured present-day spontaneous mean track length of ~14.47 μm (e.g., Donelick and Miller, 1991) and a mean induced track length of ~16.21 μm (e.g., Carlson et al., 1999), then ρ_{st} = 14.47/16.21 = 0.893. Density reduction for individual model fission-track populations is estimated using the same conversion between track length reduction and track density reduction used for population observational biasing. The correct length value to use is the one at the midpoint of a time step, rather than the end as done in Willett (1992), which biases the calculation towards lower ages and makes it unnecessarily sensitive to time step size. We estimate the midpoint length for a time step as the mean of the endpoints.

Program Interface

AFTSolve is built around the main program interface window (Fig. 2), into which t-T paths can be entered and modified and the calculated fission-track ages and length distributions displayed in real time. Time-temperature path points are introduced and moved by left-mouse-clicking and dragging of nodal points in the thermal history portion of the window; points can be deleted using the right mouse button. AFTSolve uses the Ketcham et al. (1999) annealing model as a default, but also implements the models of Laslett et al. (1987) and Crowley et al. (1991) for Durango apatite, and Crowley et al. (1991) for F-apatite.

AFTSolve also allows the user to interactively sub-divide the fission-track data into kinetic populations. Figure 3 shows the Define Kinetic Populations window, in which both the track lengths and single-grain ages are plotted against the selected kinetic parameter. The user introduces dividing lines, and the resulting pooled age and mean track length of each population is calculated and displayed. If the set of single-grain ages within a population fails the chi-squared test, the age is printed in red italics, indicating that the population is unsuitable for rigorous modeling. Up to a total of six distinct kinetic populations can be defined. Populations that are grayed by the user are not used for calculations. If more than one kinetic population is defined, the program calculates estimated fission-track ages and length distributions for each population. In addition to the fission-track solution, the AFTSolve also optionally calculates a corresponding vitrinite reflectance value using the EasyRo approach of Sweeney and Burnham (1990).

Inverse Model

AFTSolve also includes procedures that help solve the inverse problem: to determine the range of t-T paths that are consistent with a given set of fission-track data and other geological constraints. This is not strict mathematical inversion, which provides a single answer, but rather a statistical process, as a wide range of thermal histories may produce fission-track distributions that could underlie the measured data.

The components of an inverse model are a candidate t-T path generator, a statistical means of evaluating the goodness of fit between model predictions based on each t-T path generated and the measured data, and a method for searching among the various permissible t-T paths for the best-fitting solutions.

Time-temperature path generation

Candidate thermal histories are generated from user-entered constraints, which are fixed in time and require that generated t-T paths pass between two temperature extrema. Additional nodal points are generated along the t-T path between two user-entered constraints; these nodal points are equally spaced in time, in sets of 2^n-1, where n is an integer specified by the user. Each of these additional nodes are required to stay within the temperature extremes defined by the two user-entered constraints that bracket them. The user can designate maximum cooling and heating rates between all nodal points, and can force each segment of the t-T path between user-entered constraints to be monotonic (cooling or heating, depending on the relative positions of the constraints).

Merit function

We first independently evaluate the statistical goodness-of-fit of modeled fission-track length distributions and ages to the measured data. The simplest measure for evaluating the degree of fit between fission-track length distributions is the Kolmogorov-Smirnov (K-S) test (Press et al., 1988; Willett, 1992; Willett, 1997). The K-S test relies on two parameters: the maximum separation between two cumulative distribution functions (cdf) representing the measured and model track lengths, and the number of observations comprising the measured cdf. In the version of the K-S test used here, it is assumed that one cdf describes a continuous, completely known distribution, and the other describes a finite sample. The result of the test is the probability that a set of samples taken randomly from the known distribution would have a greater maximum separation from it on a cdf plot than is observed for the sample distribution being tested. Because the number of tracks counted is the statistical constraint on how well-defined the fission-track length distribution is, we assume that the model distribution is completely known and we test the measured distribution against it. For example, a K-S probability of 0.05 means that, if N random samples were taken from the distribution described by the calculation result, where N is the number of fission track lengths actually measured, there would be a 5% chance that the resulting distribution would have a greater maximum separation from the model on a cdf plot than is observed between the data and the model. The expected value for the case in which the measured track lengths are in fact samples from the model distribution is 0.5: 50% of sample populations from the model distribution would have a greater separation, and 50% would have a lesser one. The 50% limit thus marks a logical boundary of statistical precision for the track-length distribution by the K-S test.

For the fission-track age goodness of fit, we assume that the measured pooled age and its standard deviation describe the "known" distribution of possible ages and we compare the model prediction of fission-track age to this distribution. The test consists of assuming that the measured age and standard deviation describe a normal distribution, and calculating the proportion of samples from such a distribution that would be further away from the measured pooled age (i.e. analogous to the mean of the normal distribution) than the model age. The calculated probability thus has essentially the same meaning as the K-S test, only we have reversed the "known" and "sample" entities. A value of 0.05 means that 5% of possible random samples from the distribution described by the data are further away from the measured age than

the model age, and the expected value for a random sample taken from the data distribution is 0.5.

This pair of tests has the advantage that they both describe essentially the same quantity: the "probability of a worse fit." In other words, each describes the probability that, were the model t-T path truly correct and the annealing calculation accurate, a set of fission-track lengths and ages measured from a population described by the model would be less similar to the model than the data. The rough equivalence in meaning suggests that there should be no need to weight these statistics to ascribe more importance to one than the other (e.g., Corrigan, 1991; Gallagher et al., 1994).

In order to combine these two statistics into a single merit function for evaluating thermal histories against each other, we simply take their minimum (Willett, 1997). When multiple kinetic populations are being evaluated, the minimum statistic value across all populations is used.

Although it attempts to find the single t-T path that best reproduces the measured data, the primary use of AFTSolve is to define envelopes in t-T space that contain all paths that pass baseline statistical criteria and conform to user-entered constraints (Fig. 4). The first and wider envelope contains all t-T paths that have a merit function value of at least 0.05. This value is conventionally used for evaluating the null hypothesis; it can be said that models with such values "cannot be ruled out" as being sufficiently close to the data. The second envelope contains all t-T paths that have a merit function value of at least 0.5, which as discussed above can be considered as the limit of statistical precision. For ease of explanation, we term the paths and envelopes with a merit function value of 0.05 "acceptable" and fits with a merit function value of 0.5 "good". Note that not all t-T paths that fit within an envelope necessarily pass the relevant statistical requirements.

Searching algorithms

Two options are provided for searching among the t-T paths that are consistent with the user-entered constraints for ones that fit the data. The first is a Monte Carlo (MC) method, which generates and evaluates a large number of independent t-T paths. The second is an implementation of the Constrained Random Search (CRS) method (Willett, 1997), in which 250 candidate paths are generated and then combined and projected in random sets in search of the best-fitting solution. Convergence occurs after all paths have merit function values within 10^{-3} of each other. In practice, the CRS method is better when the search space is ill-constrained, and is better at locating acceptable solutions when they only traverse a limited region of t-T space, but the MC method does a better job of mapping out the full potential breadth of the t-T envelopes in well-constrained situations.

Modeling strategies

Successful use of AFTSolve for inverse modeling depends upon the careful selection of fitting conditions, principally the user-entered constraints that all t-T paths must pass through. We provide some general guidelines for where and how to set these constraints.

In general, all time-temperature histories should begin at a sufficiently high temperature to ensure that there is total annealing (i.e., no fission tracks present) as an initial condition. Thus, the earliest t-T constraint should have a minimum temperature above the total annealing temperature of the most resistant apatite being modeled. An exception to this principle might be the modeling of rapidly cooled volcanic rocks where it is known *a priori* that the initial condition is represented by zero tracks present at some temperature below the total annealing temperature. The time of the initial constraint should be somewhat earlier than the fission-track age of the most resistant kinetic population being modeled, to account for the phenomenon of age reduction by partial annealing.

The final constraint in time should correspond to the geological temperature from which the sample was collected. Another constraint might correspond to the depositional time (and temperature) of the sedimentary sequence from which the sample was obtained. If the t-T path between constraints is defined to be monotonic, additional intermediate constraints can be used to test various candidate times for heating or cooling events. Alternatively, if no monotonicity requirement is imposed, intermediate constraints can be used to increase the number of nodal points in certain parts of the path, thereby locally increasing the level of potential detail.

Both search procedures are more effective if the range of candidate time-temperature paths is restricted, which can be accomplished by using constraints with narrow temperature ranges, and forcing t-T paths to be either monotonic between constraints or have slow heating and cooling rates. However, it is also important to not enforce overly stringent restrictions such that the true t-T path is rendered unachievable. A suggested strategy is thus to start with as general a model as possible, using relatively few constraints, and progressively refine it by imposing or relaxing restrictions as suggested by successive modeling results. An example is presented below.

Example

To illustrate the capabilities of AFTSolve and how an inverse modeling investigation might proceed, we present apatite fission-track data obtained from a sample in the vicinity of the La Sal Mountains of east-central Utah, U.S.A. Sample 171-1 represents a Triassic-aged sandstone collected from the near the Colorado River base-level, the deepest accessible part of the eroded Colorado Plateau in the vicinity of the La Sal Mountains. The apatite grains from this sample span a considerable range of apatite kinetic behaviors as indicated by parameter D_{par}, as shown in the Define Populations window (Fig. 3). Two populations passing the chi-squared test are defined. The first, lower-resistance population has a midpoint D_{par} value of 1.61 μm, with a fission-track length of 11.8 ± 1.9 μm for unprojected tracks and 13.4 ± 1.3 μm for c-axis projected tracks, and an age of 19.4 ± 2.2 Ma. The population with a higher resistance to annealing, indicated by a D_{par} value of 2.94 μm, unprojected track lengths of 11.7 ± 2.1 μm and 13.6 ± 1.2 μm for *c*-axis-projected tracks, and an age of 197 ± 26 Ma. Intermediate between these end-members is a transitional set of data in that shows evidence of mixing between them, and is thus unsuitable for defining as a single population.

We first try to model this data with the CRS algorithm, using the following constraints. First, the initial temperature at 340 Ma (approximately 70% earlier than the fission-track age of the

more-resistant population) is between 235 and 245°C, far above the closure temperature of apatites having the same D_{par} parameter. The second constraint is used to signify deposition at 20 °C at 240 Ma. A third constraint is defined at 30 Ma and between 65 and 145 °C; this constraint is used to allow the temperature to rise sufficiently to allow annealing of apatites in the low-resistance population so as to result in an age near 20 Ma. The final constraint is the present-day temperature of 20 °C. Sixteen (2^4) nodal points are allowed between each pair of constraints, and the maximum heating and cooling rates between any pair of nodal points is restricted to 10 °C/m.y.

Results of this search procedure are shown in Figure 4. Figure 4a shows the fit for the entire time-temperature history, and Figure 4b shows the final 40 million years. A broad but irregular region of good fits was found by the algorithm. The irregularity reflected in Figure 4a is principally an artifact of the algorithm, and should not be interpreted too literally -- in general, there are few details that can be discerned from apatite fission-track data in the parts of t-T histories that feature rising temperatures. In Figure 4b, the t-T history appears to show evidence of two thermal peaks, one between 30-24 Ma and the other in the vicinity of 8-10 Ma. It should be noted, though, that the final part of the best-fitting region is confined to a tight trend at the maximum allowable cooling rate, which is at the margin of the broader envelope of "acceptable" results. This may be taken as an indication that the maximum cooling rate allowed is insufficient, and needs to be raised. In general, model results where envelopes coincide with maximum rates or constraint boundaries can be taken as a sign that the relevant restrictions should be relaxed.

Figure 5 shows the results of a second model run with identical conditions as the first, save that the maximum allowable cooling rate was raised to 20 °C/m.y. The early part of the thermal history is similar, although the irregularities do not correspond with the those of the previous model. In this case, the late-stage thermal history appears not to have been as confined by the cooling rate restriction, so we can assume that the fitting conditions are reasonable. The range spanned by the "good" envelopes in the late-stage history is somewhat broader, owing to the fact that a larger range of possibilities has arisen because of the relaxation of fitting restrictions. There is still evidence of a thermal high between 30 and 24 Ma, but the later thermal high implied in the previous model is not as clear.

The previous models were based on using c-axis-projected fission-track length data, which is a novelty in comparison with earlier modeling programs and calibrations based on non-projected track lengths. Figure 6 shows the result of a model based on mean fission-tracks length that is otherwise equivalent to that shown in Figure 5b. A broader envelope of statistically good fits to the data has been found, reflecting a reduction in the resolution of the fission-track data when modeled in this way. Because c-axis projection removes part of the spread of the data caused by annealing and etching anisotropy, model results must fit the data much more closely to achieve statistically equivalent results.

Because the CRS algorithm is geared to finding the best-fitting solution, it is not optimal for determining the full extent of the envelope of statistically acceptable solutions. To obtain a more complete solution, a Monte Carlo approach is used. Figure 7 shows the results for a model based on the same criteria as that shown in Figure 5, only using MC inversion. The irregular shape of the envelope of good solutions is caused by the fact that only two such solutions were found in

50,000 independent random paths. However, the range of statistically acceptable models is much broader than previously calculated.

One characteristic of all of these inversions that can be observed in the best-fitting paths is that the flexibility of the fitting criteria allows thermal histories to feature numerous minor highs and lows. Though this is not necessarily incorrect, it is contrary to the usual way of considering geological histories as consisting of comparatively few large and influential events, such as magmatism and tectonism, which subsequently determine the evolution of temperatures for long periods of time. In order to restrict the range of possible t-T histories to ones that adhere to such considerations, one can place constraints at all presumed thermal minima and maxima, and require that all path segments between constraints must be monotonic.

The CRS algorithm in AFTSolve is not yet well-suited for working with monotonic t-T paths, as the extent of averaging employed by the technique makes such paths tend to be rather gradually changing, diminishing the possibility of generating paths with sudden changes in slope. As a result, in many cases a Monte Carlo approach will be more successful. Alternatively, additional constraints can be imposed on a CRS model at the times of probable sudden shifts in heating or cooling rates. The result of such a model is shown in Figure 8. The constraint that was previously at 30 Ma has been moved to 26 Ma to mark a candidate time for peak late heating, and additional constraints have been imposed based on insight gained from previous modeling about potential locations of sudden changes in the t-T path slope. The resulting history envelopes are much more narrow than previously calculated, primarily because of the requirement for monotonic paths.

From the modeling of sample 171-1, the following insights can be gained.   The thermal high between 30 and 24 Ma corresponds closely to the timing of the ca. 25-28 Ma La Sal Mountain shallow intrusive complex (Nelson et al., 1992, and references therein). After reaching peak temperature, it probably remained at relatively high temperature or cooled fairly slowly until rapid late-stage cooling, probably due to uplift and erosion of the Colorado Plateau. Conventional modeling of the fission-track data from this sample would lack the resolution offered by the kinetic parameter (in this case D_{par}) and would likely provide an erroneous thermal history interpretation.

Suggestions for reporting results

In general, when reporting results from AFTSolve it is good practice to include all modeling parameters used. Tables 1 and 2 are examples based on the modeling in this paper. Table 1 lists the populations that were defined from the data set, and their respective kinetic parameters, ages, lengths, and numbers of measurements. Table 2 lists the parameters used to generate and search among candidate t-T histories. AFTSolve includes utilities that facilitate the generation of these reports. In addition to the data in the tables, it is also necessary to report the annealing model used, the length type modeled (l_c or l_m), and whether Cf-irradiation was employed and taken into account by the program.

Availability

AFTSolve was written originally for Windows 3.1 in Borland Turbo C++, and although it remains a 16-bit program it has been tested and successfully run on computers running Windows 95, Windows 98, and Windows NT 4.0. It is downloadable as a self-extracting archive which includes the executable file, a necessary library, example files, and documentation. AFTSolve is available free of charge to all not-for-profit educational institutions when used for non-for-profit research purposes. Academic inquiries should be directed to Richard A. Ketcham; inquiries regarding the commercial use of AFTSolve should be directed to Raymond A. Donelick.

Acknowledgments

Table 1: Fission-track kinetic populations for sample 171-1.

Sample	Pop	D_{par} Range (μm)	Model D_{par} (μm)	Model l_0 (μm)	Age (Ma [N])	Length (μm [N])
	1	1.27-1.97	1.61	16.43	19.4±2.2 [24]	13.4±1.3 [119]
171-1	2	1.97-2.60	2.27	16.57	58.1±6.9 [8]	12.9±1.7 [52]
	3	2.60-3.25	2.94	16.70	197±26 [8]	13.6±1.2 [16]

Table 2: Modeling parameters used for results presented in this paper.

Model	Sample	Pops	Constraints: (Ma, °C-°C)	Search Mode	Iter.	Nodal Points	Max. dT/dt (°C/Ma)	Mono?
1	171-1	1,3	(0, 20-20) (30, 144-65) (241, 21-17) (337, 246-232)	CRS	10250	49	+10/-10	N
2	171-1	1,3	(0, 20-20) (30, 144-65) (241, 21-17) (337, 246-232)	CRS	10250	49	+10/-20	N
3	171-1	1,3	(0, 20-20) (30, 144-65) (241, 21-17) (337, 246-232)	CRS	10250	49	+10/-20	N
4	171-1	1,3	(0, 20-20) (30, 144-65) (241, 21-17) (337, 246-232)	MC	50000	49	+10/-20	N
5	171-1	1,3	(0, 17-16) (3, 88-38) (26, 140-79) (107, 63-17) (241, 16-16) (298, 246-232)	CRS	10250	41	N.A.	Y

Pops: which populations from sample data were modeled; Search Mode: CRS = Constrained Random Search, MC = Monte Carlo; Iter.: number of iterations used to search for solutions; Mono?: Y = time-temperature paths between constraints forced to be monotonic.

$$\sigma_{c,mod} = 0.008452 * L_{c,mod}^2 - 0.2442 * L_{c,mod} + 2.312$$

$$\sigma_m = 0.02858 * L_m^2 - 0.8733 * L_m + 7.464$$
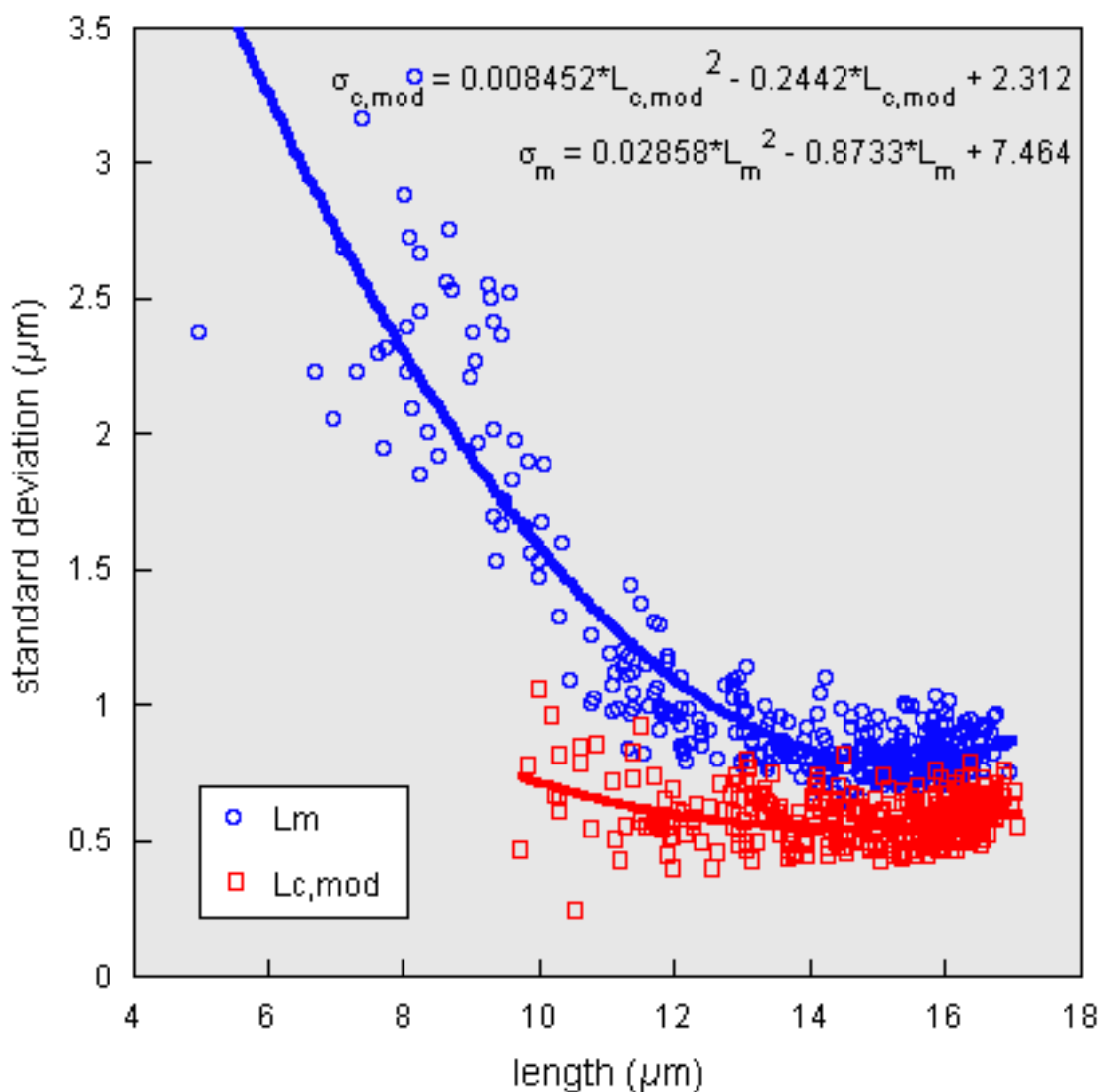
Figure 1. Functions relating modeled fission-track lengths to estimated spread in lengths for non-projected and *c*-axis-projected fission tracks.   After calculation of a fission-track length using an annealing calibration, these functions are used to complete the description of the distribution of fission tracks that would be observed. The removal of annealing and etching anisotropy from track length measurements by *c*-axis projection results in tighter distributions, leading to better resolution ability.
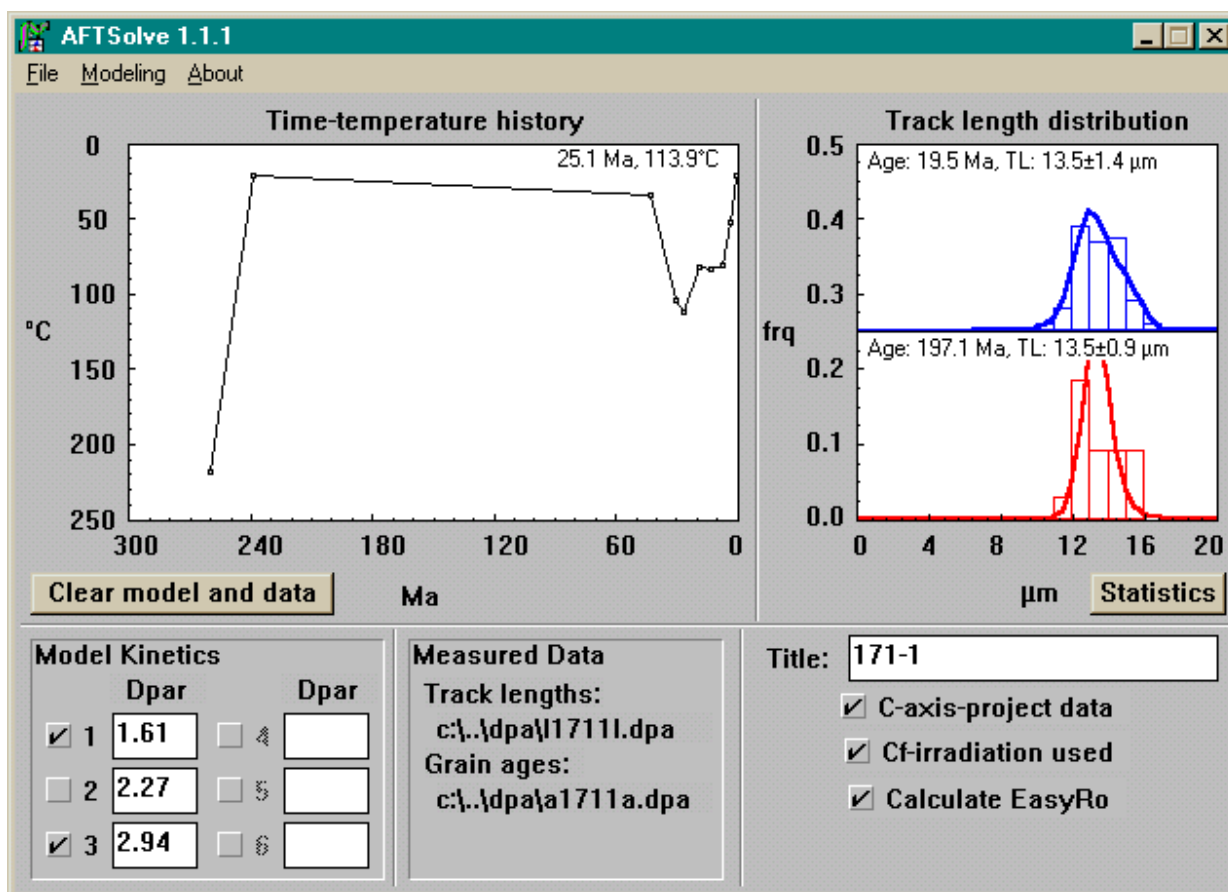
Figure 2. AFTSolve main program interface window. The upper-left graph is used for entering and displaying time-temperature histories; time-temperature nodal points can be added and deleted using mouse clicks. The upper-right graph is used for displaying model results; histograms show measured track length data, and continuous curves show model-generated track-length distributions. In this case two kinetic populations are being modeled; the upper blue model is for the population that is less resistant to annealing, and the lower red model is for the more resistant population.
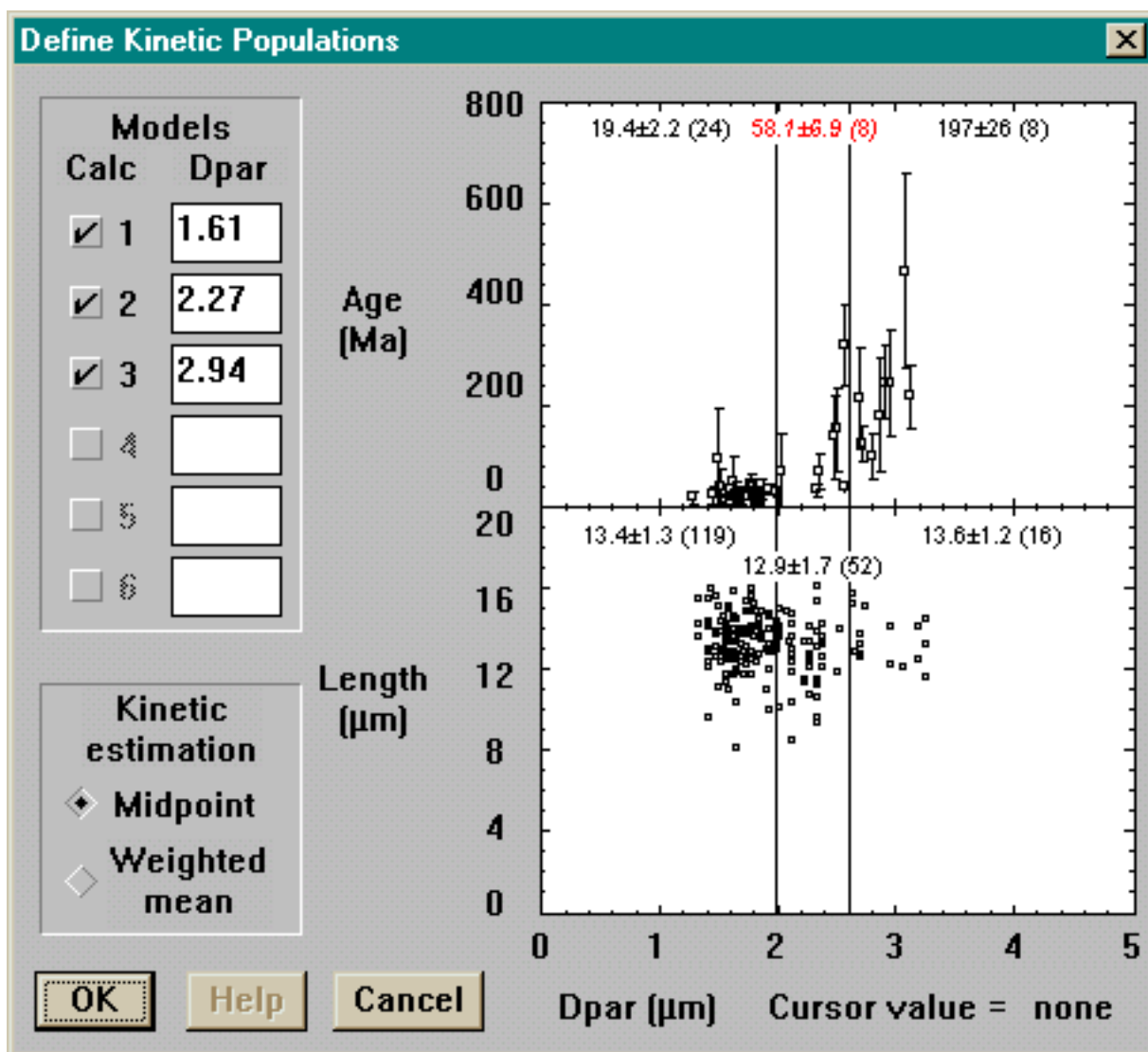
Figure 3. AFTSolve interface for dividing apatite grains into distinct kinetic populations. The horizontal axis of the dual graph on the right is the kinetic parameter, in this case D_{par}. Upper graph on right shows single-grain ages with one-sigma error bars, and lower graph on right shows track lengths. Headings on graphs show pooled ages and mean track lengths for each population. The red italics for the pooled age for the middle population indicates that the single-grain ages do not pass the chi-squared test, and that this population is thus unsuitable for inverse modeling. For the modeling in this paper, the end-member populations are used instead.
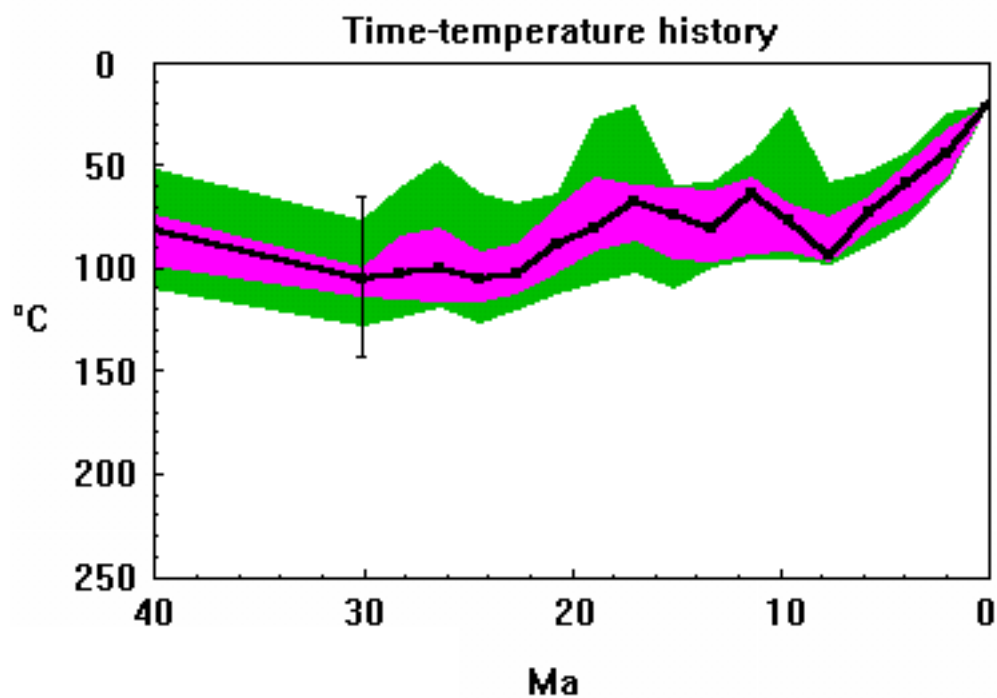
A.
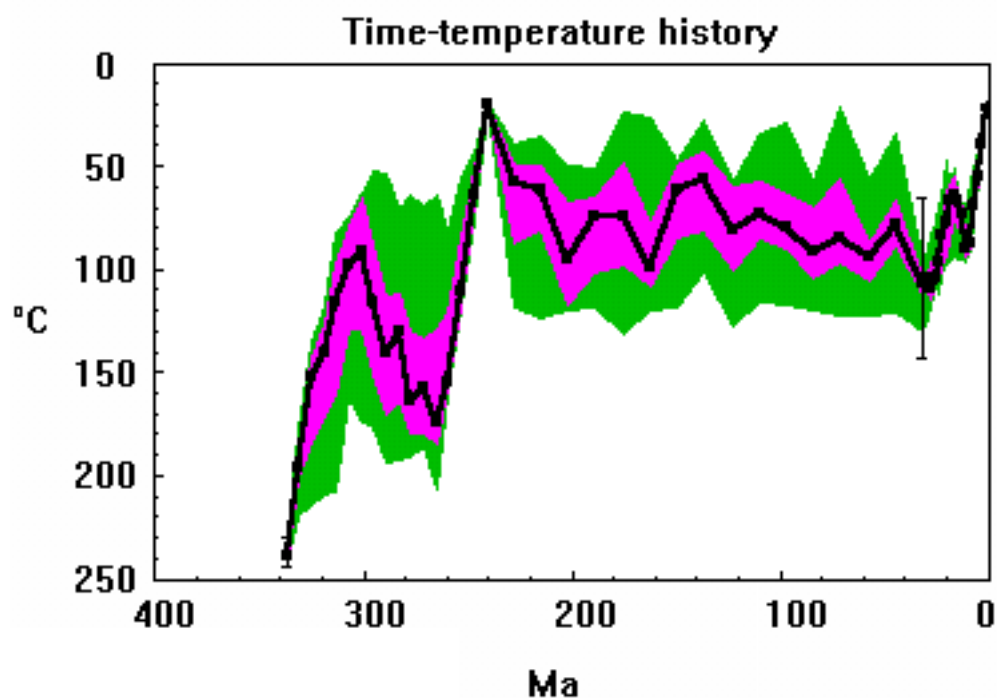
B.
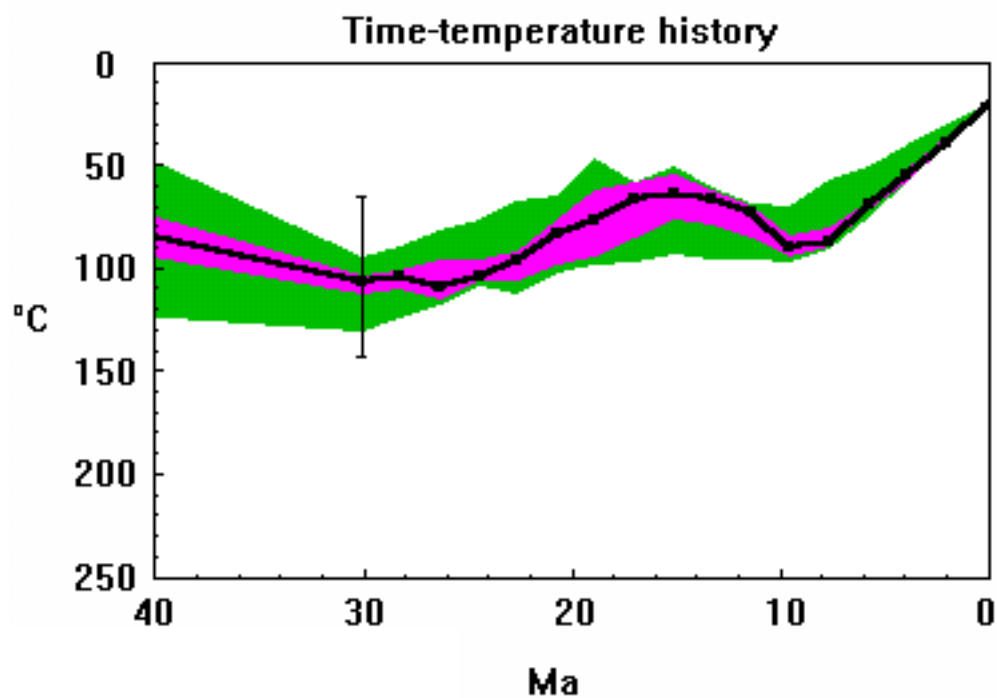
Figure 4. First attempt at inverse model of time-temperature history for sample 171-1. Green regions mark envelopes of statistically acceptable fits. Magenta regions bound envelopes for statistically good fits. I-bars mark user-entered time-temperature constraints. Thick line marks the best-fitting t-T path found.
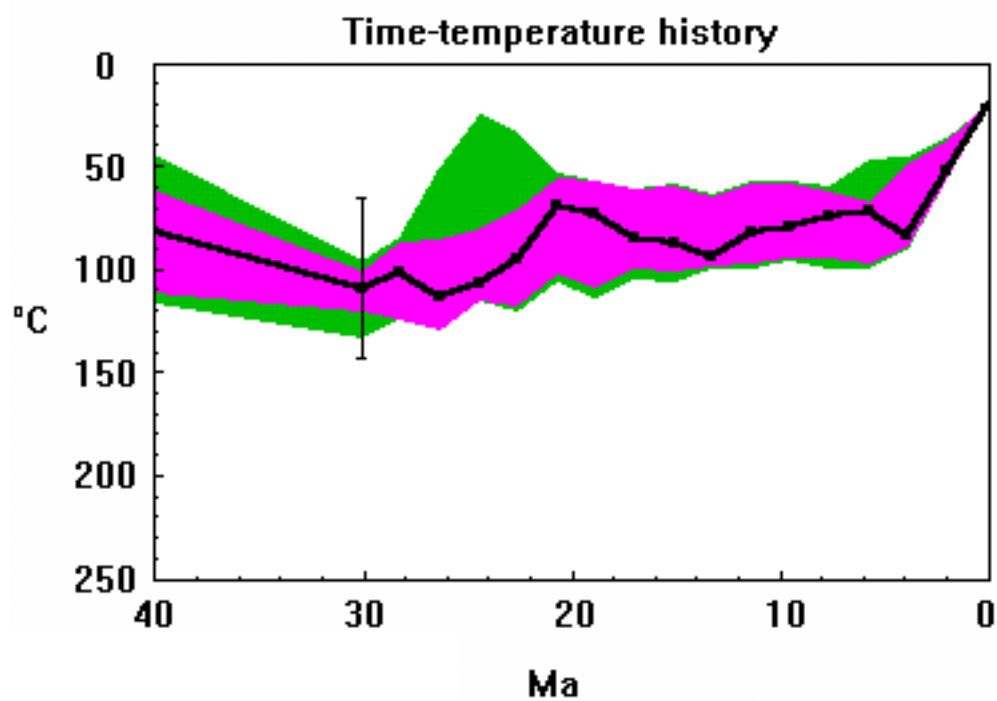
A.
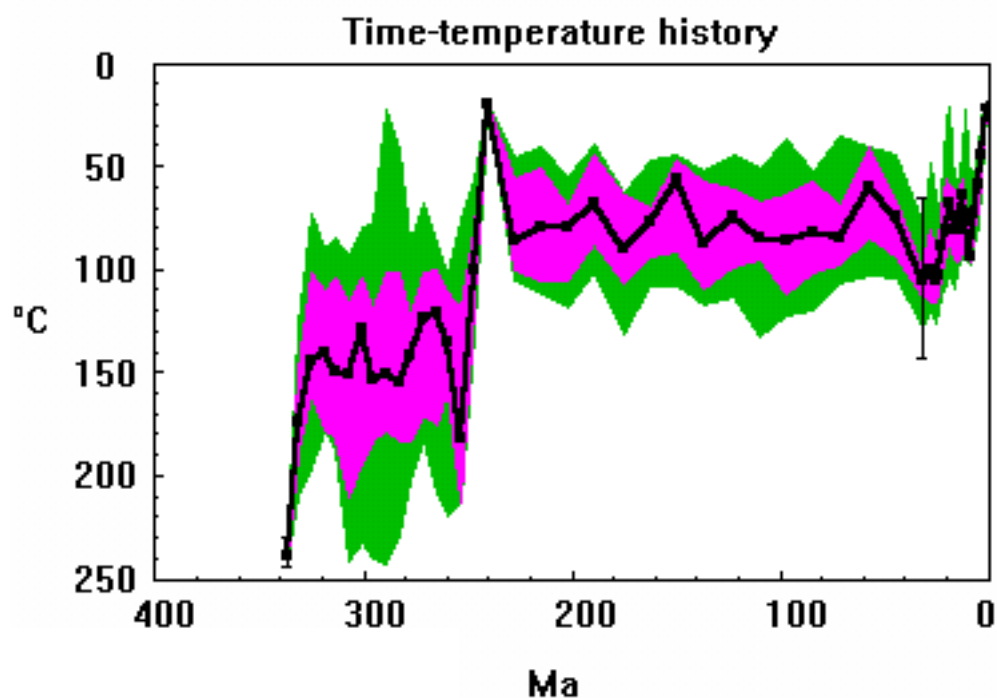
B.

Figure 5. Second attempt at inverse model. By allowing faster cooling rates to accommodate the apparent requirement for rapid late-stage cooling, a wider selection of statistically good fits has been found.
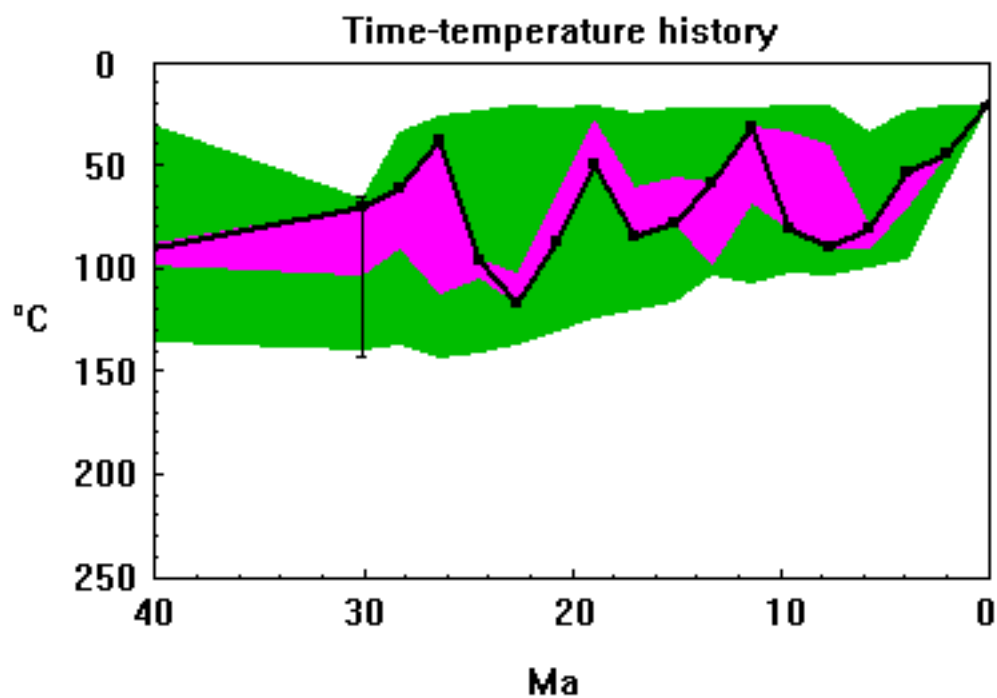
Figure 6. Inverse model based on mean fission-track lengths rather than *c*-axis-projected lengths. The wider range of statistically good fits reflects a reduction in the resolving ability of the data.

A.
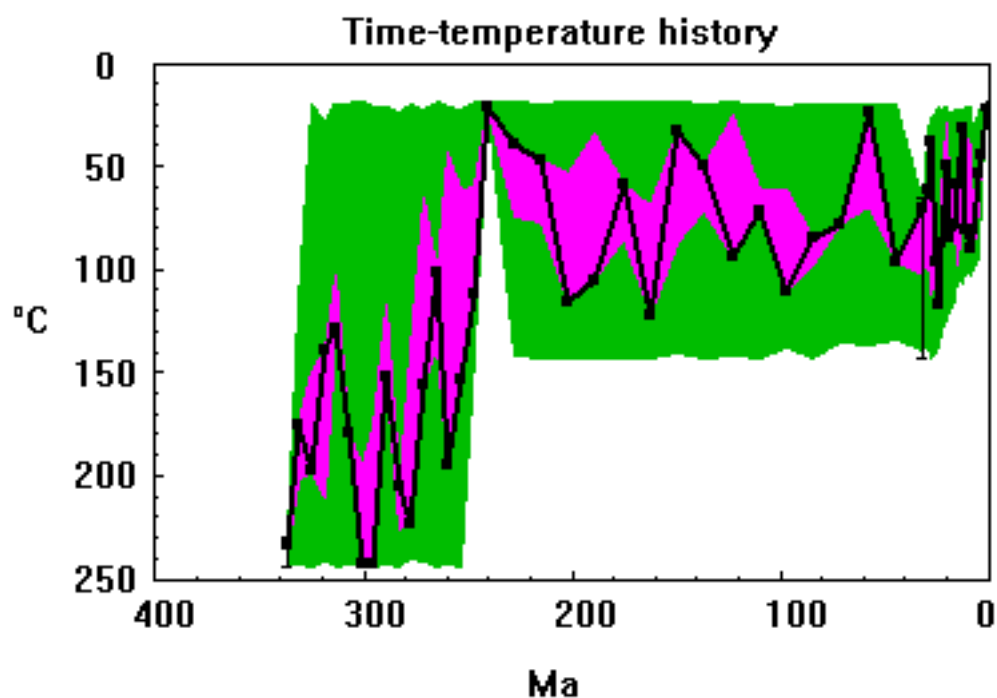
B.
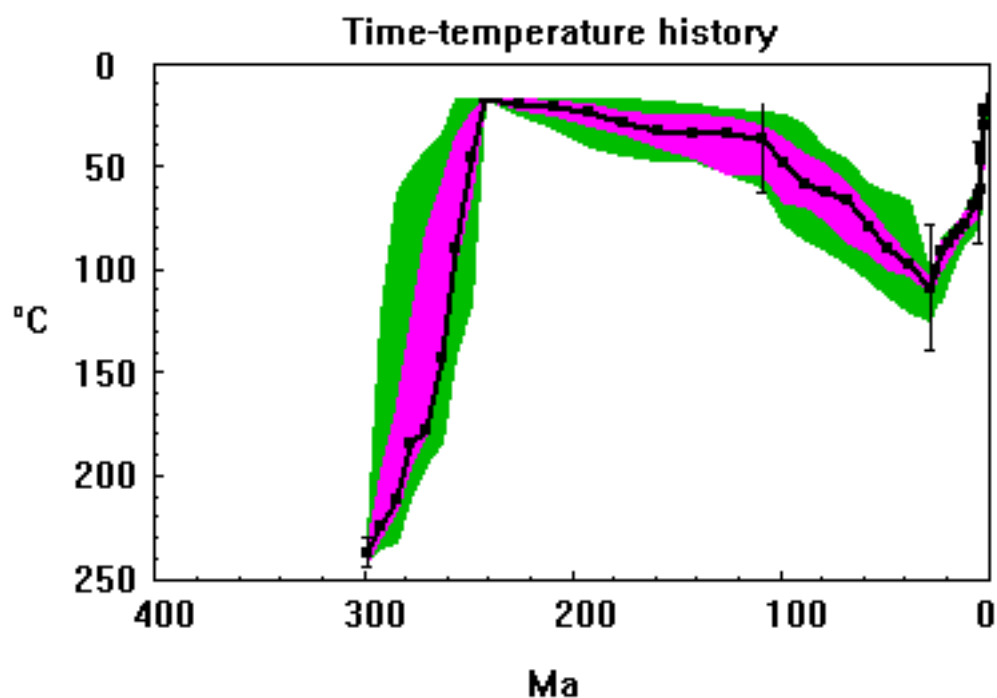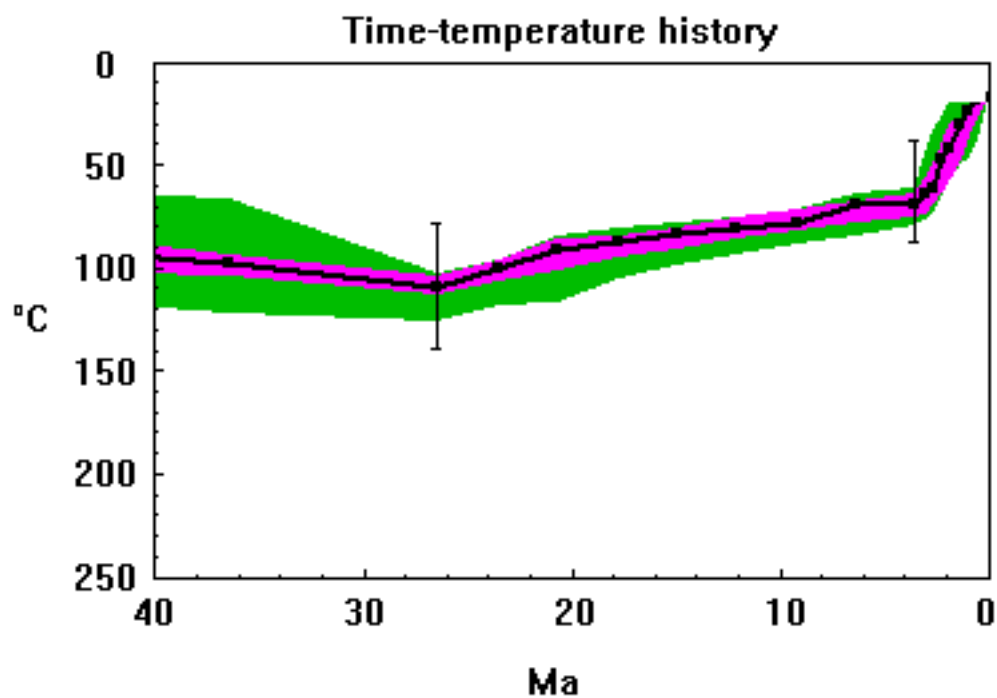

Figure 7. Inverse models based on 50,000 independently generated t-T paths using Monte Carlo method. The range of statistically acceptable solutions found is much broader than that found using the CRS method. However, fewer statistically good fits have been found. Additionally, the complexity of t-T paths permitted by the fitting criteria may be unrealistic.

A.

B.

Figure 8. Results of inversion assuming t-T paths are monotonic between user-imposed constraints. The range of thermal histories compatible with the data under these conditions is much more restricted.

References cited

Burtner, R.L., Nigrini, A., and Donelick, R.A. (1994) Thermochronology of lower Cretaceous source rocks in the Idaho-Wyoming thrust belt. American Association of Petroleum Geologists Bulletin, 78(10), 1613-1636.

Carlson, W.D. (1990) Mechanisms and kinetics of apatite fission-track annealing. American Mineralogist, 75, 1120-1139.

Carlson, W.D., Donelick, R.A., and Ketcham, R.A. (1999) Variability of apatite fission-track annealing kinetics I: Experimental results. American Mineralogist, 84, 1213-1223.

Corrigan, J.D. (1991) Inversion of apatite fission track data for thermal history information. Journal of Geophysical Research, 96, 10347-10360.

Crowley, K.D. (1993) Lenmodel: a forward model for calculating length distributions and fission-track ages in apatite. Computers and Geosciences, 19, 619-626.

Crowley, K.D., Cameron, M., and Schaefer, R.L. (1991) Experimental studies of annealing etched fission tracks in fluorapatite. Geochimica et Cosmochimica Acta, 55, 1449-1465.

Donelick, R.A. (1993) A method of fission track analysis utilizing bulk chemical etching of apatite, U.S.

Donelick, R.A. (1995) A method of fission track analysis utilizing bulk chemical etching of apatite, Australia.

Donelick, R.A., Ketcham, R.A., and Carlson, W.D. (1999) Variability of apatite fission-track annealing kinetics II: Crystallographic orientation effects. American Mineralogist, 84, 1224-1234.

Donelick, R.A., and Miller, D.S. (1991) Enhanced TINT fission track densities in low spontaneous track density apatites using 252Cf-derived fission fragment tracks: A model and experimental observations. Nuclear Tracks and Radiation Measurements, 18, 301-307.

Gallagher, K. (1995) Evolving temperature histories from apatite fission-track data. Earth and Planetary Science Letters, 136, 421-435.

Gallagher, K., Hawkesworth, C.J., and Mantovani, M.S.M. (1994) The denudation history of the onshore continental margin of SE Brazil inferred from apatite fission track data. Journal of Geophysical Research, 99, 18117-18145.

Green, P.F. (1988) The relationship between track shortening and fission track age reduction in apatite: Combined influences of inherent instability, annealing anisotropy, length bias and system calibration. Earth and Planetary Science Letters, 89, 335-352.

Green, P.F., Duddy, I.R., Gleadow, A.J.W., and Lovering, J.F. (1989) Apatite fission-track analysis as a paleotemperature indicator for hydrocarbon exploration. In N.D. Naeser, and T.H. McCulloh, Eds. Thermal Histories of Sedimentary Basins: Methods and Case Histories, p. 181-195. Springer, New York.

Green, P.F., Duddy, I.R., Gleadow, A.J.W., Tingate, P.R., and Laslett, G.M. (1986) Thermal annealing of fission tracks in apatite 1. A qualitative description. Chemical Geology (Isotope Geoscience Section), 59, 237-253.

Issler, D.R. (1996) Optimizing time step size for apatite fission track annealing models. Computers and Geosciences, 22, 67-74.

Ketcham, R.A., Donelick, R.A., and Carlson, W.D. (1999) Variability of apatite fission-track annealing kinetics III: Extrapolation to geological time scales. American Mineralogist, 84, 1235-1255.

Laslett, G.M., and Galbraith, R.F. (1996) Statistical modelling of thermal annealing of fission tracks in apatite. Geochimica et Cosmochimica Acta, 60, 5117-5131.

Laslett, G.M., Green, P.F., Duddy, I.R., and Gleadow, A.J.W. (1987) Thermal annealing of fission tracks in apatite 2. A quantitative analysis. Chemical Geology   (Isotope Geoscience Section), 65, 1-13.

Laslett, G.M., Kendall, W.S., Gleadow, A.J.W., and Duddy, I.R. (1982) Bias in measurement of fission-track length distributions. Nuclear Tracks and Radiation Measurements, 6, 79-85.

Lutz, T.M., and Omar, G. (1991) An inverse method of modeling thermal histories from apatite fission-track data. Earth and Planetary Science Letters, 104, 181-195.

Nelson, S.T., Davidson, J.P., and Sullivan, K.R. (1992) New age determinations of central Colorado Plateau laccoliths, Utah: Recognizing disturbed K-Ar systematics and re-evaluating tectonomagmatic relationships. Geological Society of America Bulletin, 104, 1547-1560.

Press, W.H., Flannery, B.P., Teukolsky, S.A., and Vettering, W.T. (1988) Numerical Recipes in C. 735 p. Cambridge University Press, Cambridge.

Sweeney, J.J., and Burnham, A.K. (1990) Evaluation of a simple model of vitrinite reflectance based on chemical kinetics. American Association of Petroleum Geologists Bulletin, 74, 1559-1670.

Vrolijk, P., Donelick, R.A., Queng, J., and Cloos, M. (1992) Testing models of fission track annealing in apatite in a simple thermal setting: site 800, leg 129. In R.L. Larson, and Y. Lancelot, Eds. Proceedings of the Ocean Drilling Program, Scientific Results, 129, p. 169-176.

Willett, S.D. (1992) Modelling thermal annealing of fission tracks in apatite. In M. Zentilli, and P.H. Reynolds, Eds. Short Course Handbook on Low Temperature Thermochronology, p. 43-72. Mineralogical Association of Canada.

Willett, S.D. (1997) Inverse modeling of annealing of fission tracks in apatite 1: A controlled random search methodAmerican. American Journal of Science, 297, 939-969.